Desalination and Water Treatment
www.deswater.com

doi: 10.5004/dwt.2018.22360

118 (2018) 163–171
June

Evaluation of modified chitosan nanoparticles as sorbent for chromium(VI) ions from polluted water

Naifa S. Alatawi[a], Nadia H. Elsayed[b,c], W.S. Mohamed[c,*]

[a]*Physics Department, Faculty of Science, University of Tabuk, Tabuk 71421, Saudi Arabia, email: goood_28@hotmail.com*
[b]*Chemistry Department, Faculty of Science, University of Tabuk, Tabuk 71421, Saudi Arabia, email: nhelsayed@ut.edu.sa*
[c]*Department of Polymers and Pigments, National Research Centre, Cairo 12311, Egypt,*
email: ws.mohamed@nrc.sci.eg (W.S. Mohamed)

Received 9 December 2017; Accepted 8 April 2018

ABSTRACT

Chitosan nanoparticles with particle size about 84 nm were successfully prepared in tripolyphosphate (TPP) solution and modified through redox grafting reaction of different amounts of amino ethyl methacrylate (AEMA) monomer producing chitosan-*g*-AEMA. Both of chitosan and its modified copolymer were characterized by Fourier-transform infrared, scanning electron microscopy and transmission electronic microscopy analyses. The prepared chitosan and chitosan-*g*-AEMA were used for adsorption of Cr(VI). The effect of pH values, adsorbent dose, contact time, temperature and Cr(VI) ion concentration was studied. The data show that the percentage of Cr(VI) removal using chitosan-*g*-AEMA is more than that of chitosan nanoparticles. The optimum conditions for adsorption of Cr(VI) were pH 3 and 120 min of contact time at room temperature using 2:1 chitosan:AEMA ratio. Adsorption process was confirmed by Langmuir's model.

Keywords: Chitosan nanoparticles; AEMA; Adsorption; Chromium

1. Introduction

Pollutants including heavy metals such as Cr, Pb and Ni enter into our food through water contaminations with a negative effect on the life of living organisms [1]. According to Hoffmann et al. [2], 70% of the water resources containing toxic chemicals are considered to be the main source of water contaminations.

Chitosan is a highly basic polysaccharides with high chelating ability [3] and considered to be the most numerous carbohydrate biopolymers which are characterized by its non-toxicity and biodegradability properties. It can be extracted from shrimps and can be prepared in nano-form for using in different applications as drug delivery, and anti-microbial activities. In addition, chitosan is suitable for removing heavy metals by adsorption by modifiable positions in its chemical structure [4].

Chitosan has a high adsorption capacity due to the presence of nitrogen content in a form of a primary amino group. Recently, an attention has been focused on the nanoadsorbents due to its high surface area and permeability which enhance the adsorption capacity. Many efforts have been carried out for modification of chitosan in order to increasing its adsorption capacity [5].

Metal ion adsorption from aqueous solutions can be achieved through different techniques such as metal precipitation, electro-deposition, ion-exchange and membrane formation [6]. Metal ion adsorption capacity of chitosan could be improved via incorporation of additive function groups to chitosan structure through grafting reaction [7]. Grafting polymerization of acrylate monomers as acrylic acid [8] and methyl methacrylate (MMA) [9] monomers onto chitosan backbone via chemical or radiation initiation systems is considered as one of the hopeful attempts for increasing the chitosan adsorption efficiency [10]. Chitosan–MMA nanoparticles can be prepared by grafting of MMA onto chitosan and gave good results in metal adsorption [11].

---

* Corresponding author.

1944-3994/1944-3986

Pollution by chromium in water resources through such industries like dyes, pigments, electro-plating and tanning is a more dangerous behavior [12,13]. Chromium in water is present in two forms Cr(III) and Cr(VI) ions where the second form is highly soluble, more toxic and dangerous due to fast diffusion ability through cell membrane to form $(CrO_4)^{2-}$ and $(HCRO_4)^-$ [14]. The negative effect of Cr(VI) could be minimized by conversion into Cr(III) through biological or chemical reduction processes [15].

Reverse osmosis, solvent extraction and chemical precipitation are used for removing Cr(VI) from water. The most efficient method was adsorption method using zeolite [16] and graphene [17]. Different adsorbent had been used for removal of Cr(VI) such as magnetically modified graphene oxide–chitosan composite [18], amino terminated hyperbranched dendritic polyamidoamine third generation chitosan beads [19], and chitosan grafted with *n*-butylacrylate [20]. Chitosan modified-bioreduced non-tronite [21], beta-cyclodextrin–chitosan modified walnut shell biochars [14], chitosan modified with epichlorohydrin [22], graphene oxide–chitosan composite [23] and chitosan modified with polyalginic acid [3] give good results for removal of Cr(VI).

The aim of the work is to prepare chitosan nanoparticles modified with poly(AEMA) via redox grafting polymerization process in order to compare the efficacy of the prepared chitosan nanoparticles with its poly(AEMA) graft copolymer in Cr(VI) adsorption from water samples in different reaction and environmental conditions.

2. Experimental

2.1. Materials

Chitosan, powder acetylation degree 14%, viscosity average molecular weight 40,000 kDa and amino ethyl methacrylate (AEMA) monomers were supplied by Fluka Chemical, Germany. Potassium persulfate initiator (KPS), sodium bisulfate (NaBS), sodium hydroxide, hydrochloric acid and glacial acetic acid were purchased from El-Nasr Company, Egypt. Sodium tripolyphosphate (TPP) $Na_5P_3O_{10}$ technical grade, 85% with molecular weight 367.86 was purchased from Sigma-Aldrich, Germany. Sodium TPP solution was prepared using bidistilled water.

2.2. Preparation of chitosan nanoparticles

Chitosan was in 1% acetic acid. The pH is adjusted to 4.6–4.8 using sodium hydroxide. 1 mL of 0.25% sodium TTP solution was added to 3 mL of chitosan solution under magnetic stirring chitosan nanoparticles was shaped spontaneously [24]. The formed nanoparticles were purified by centrifugation at 9,000 rpm for 30 min. Supernatants were discarded, and the chitosan nanoparticles were extensively rinsed with deionized distilled water to remove any sodium hydroxide and thereafter freeze-dried before further use or analysis.

2.3. Preparation of chitosan-g-poly(AEMA)

The grafting of the AEMA monomer onto the chitosan backbone was done by KPS/NaBS redox initiation method [25]. 100 mL of 1% acetic acid solution was prepared in a 250 mL flask, 0.4 g of chitosan was added with shaking at 100 rpm for about 30 min. KPS/NaBS redox initiation system (with ratio 10:20 mmol) was added slowly to the reaction flask. During stirring process with a desired amount of acidified AEMA solution (pH 4 ± 0.2 with nitric acid) and the mixture was allowed to react for 2 h in a thermostatic water bath. During the reaction time the temperature was allowed to increase gradually following the 50°C for 30 min; 60°C for 30 min and finally 70°C for 60 min. The reaction mixture was allowed to precipitate in ethyl alcohol/water (80/20). A white precipitate in the form of copolymer was allowed to wash with excess acetone many times, to remove any homopolymer. The copolymer was dried in a vacuum oven at 50°C for 24 h. The solid contents of the obtained copolymers were determined gravimetrically.

2.4. Effect of grafting ratio

The optimal grafting ratio which was determined by grafting yield calculation using the following equation [26]:

$$\text{G.Y. (\%)} = [(W_1 - W_2)/W_1] \times 100 \tag{1}$$

where W_1 and W_2 are the weight of chitosan before and after grafting, respectively.

The effect of grafting ratio was studied to determine the effect of chitosan/monomer ratio in the grafting percentage where chitosan/AEMA ratios were 1:1, 2:1, 3:1 and 5:1.

2.5. Polymer characterization

Fourier-transform infrared (FTIR) spectra of chitosan and chitosan-*g*-AEMA were recorded on a FTIR spectrophotometer (Thermo Nicolet, NEXUS, TM) in the range of 4,000–400 cm^{-1} using KBr pellets.

Chitosan and chitosan-*g*-AEMA samples were analyzed by thermal gravimetric analysis. A solid sample (5 mg) was placed on a thin platinum pan and was conducted at a heat flow rate of 10°C/min under purging nitrogen for thermal gravimetric measurement. The temperature range of measurement was varied between 30°C and 600°C.

The particle size of the chitosan nanoparticles was measured by transmission electronic microscopy (TEM), where the TEM images were obtained by JEM-1230-electron microscopy operated at 60 kV. A drop of well dispersed diluted sample was placed onto a copper grid (200 mesh and covered with a carbon membrane) and dried at ambient temperature.

The morphology of the chitosan and chitosan-*g*-AEMA samples was investigated using scanning electron microscope (SEM). SEM images were obtained by JEOL Model JSM-T20 SEM.

2.6. Preparation of aqueous solutions of Cr(VI) ions

A stock solution of Cr(VI) solutions was prepared from stock solution of K_2CrO_4 (0.1 M) by successive dilution with double distilled water [27]. Different concentration of Cr(VI) solutions (1×10^{-2}, 1×10^{-3} and 1×10^{-4} mol L^{-1}) were prepared by dilution and used for performing the chemical deposition

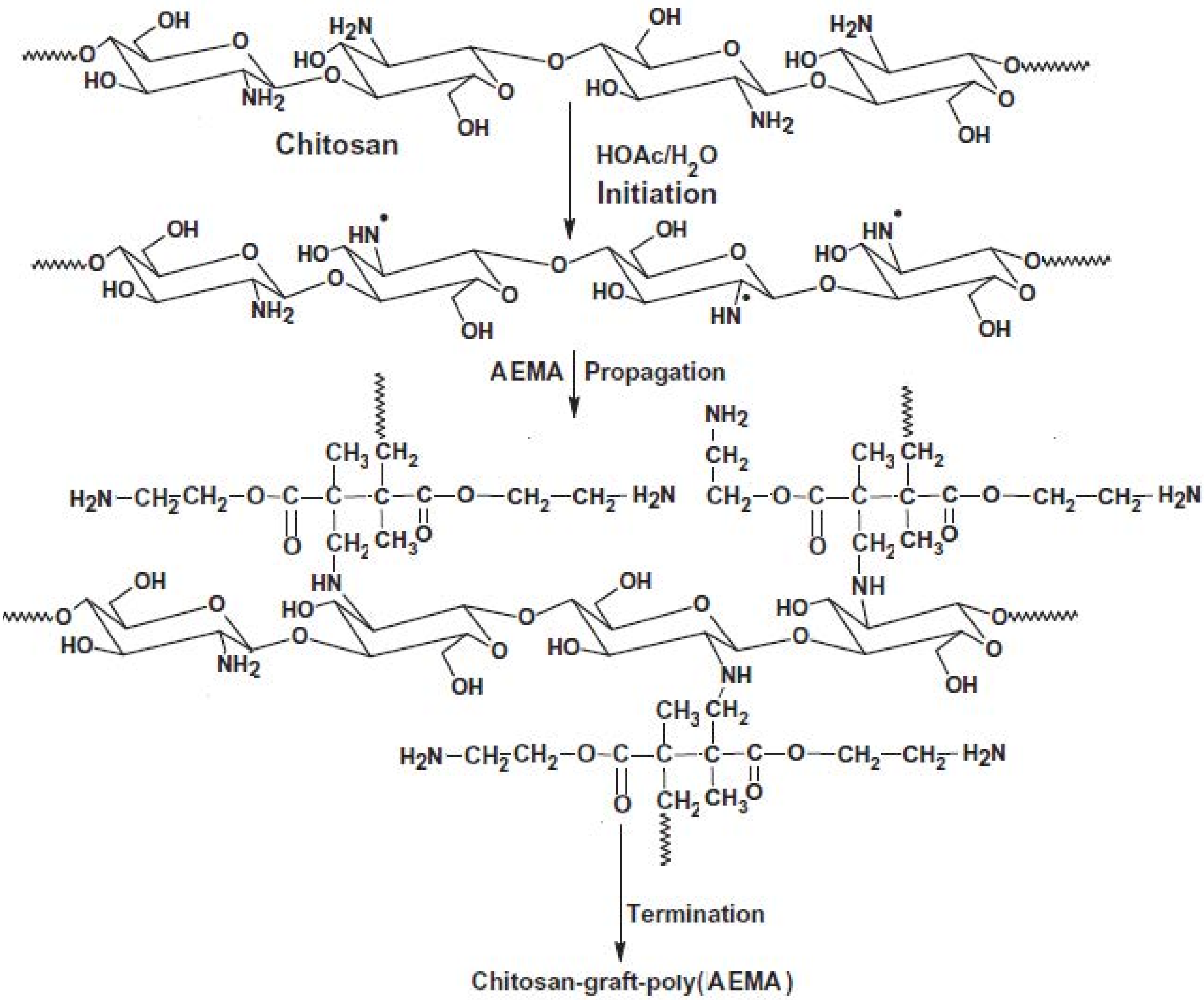

Fig. 1. Grafting mechanism of AEMA onto chitosan.

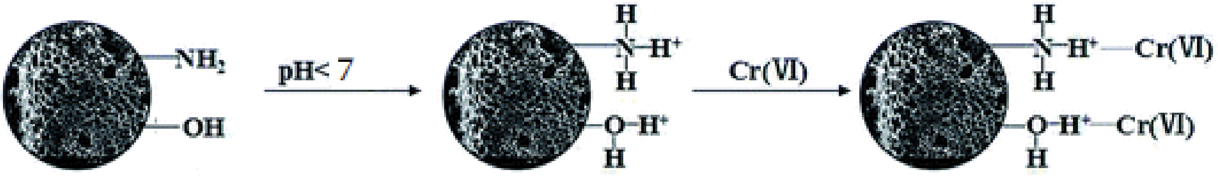

Fig. 2. Cr(VI) removal mechanism using chitosan and chitosan-*g*-AEMA.

experiments. The pH of solutions was adjusted by using 0.1 M HCl or NaOH solution.

2.7. Adsorption experiments

Different doses of dry adsorbent were placed in 150 mL stoppard flask containing 100 mL aqueous solution of different concentrations of Cr(VI). A thermostatic shaker with velocity of 200 rpm was used for different samples for specific time (15–180 min) at the desired temperature (25°C–50°C). The effect of pH on the adsorbed metal ions was studied at the range 2–8.

The remaining concentrations of the Cr metal ion in the solutions after adsorption were analyzed using a Shimadzu atomic absorption spectrophotometer (AA-6650) and the removal efficiency (E%) is calculated using the following equation [28]:

$$\text{The removal efficiency } (E\%) = (C_i - C_f)/C_i \times 100...... \quad (2)$$

where C_i and C_f are the initial and remaining concentrations of the metal ions, respectively.

3. Results and discussion

3.1. Characterization of chitosan nanoparticles and chitosan-g-AEMA

Chitosan nanoparticles were prepared based on the reaction at room temperature between positive charge chitosan and negative charge TTP.

Chitosan-*g*-AEMA was prepared by grafting of AEMA monomer onto chitosan nanoparticle in 3:1 mole ratio in the presence of KPS/NaBS redox initiation system.

The products were characterized by SEM, TEM, FTIR and X-ray diffraction analyses.

The SEM micrographs of Fig. 3 show spherical shape and high distribution of chitosan nanoparticles of the prepared chitosan and chitosan-*g*-AEMA. AEMA grafting successfully indicated by the presence of polymer particles on the chitosan surface.

The particle size of the prepared chitosan nanoparticles was determined by TEM analysis (Fig. 4). It is clear that the prepared chitosan has high dispersion in acidic solution and the particle size lies in the range of 84 nm.

Fig. 4 also indicates the successful grafting of AEMA monomer onto chitosan with uniform distribution of grafted polymer on the chitosan surface.

FTIR analysis [29] of the prepared chitosan nanoparticles is shown in Fig. 5. It is clear that the bands related to chitosan (N–H) and (O–H) groups were assigned in the range 3,457 cm^{-1} where the bands at 2,880 and 1,440 cm^{-1} are related to (C–H) and (C–N) groups, respectively. The presence of bands characteristic for C=O and C–H alkenes was assigned in 1,760 and 3,100 cm^{-1}, respectively. FTIR analysis of chitosan-*g*-AEMA confirms the successful grafting of AEMA monomer onto chitosan surface.

A characteristic peaks of Cr–O and Cr=O at 750 and 940 cm^{-1} was detected in the FTIR analysis of chitosan-*g*-AEMA loaded Cr(VI) which confirm the successful loading of Cr(VI) onto chitosan-*g*-AEMA [30].

The thermal stability of the prepared chitosan and chitosan-*g*-AEMA samples was determined by thermogravimetric analysis (TGA) within the temperature range 50°C–650°C (Fig. 6). The data related to the temperature degradation at which weight loss starting temperature (T_{start}), 10% weight loss temperature (T_{10}), 25% weight loss temperature (T_{25}), 50% weight loss temperature (T_{50}), 75% weight loss temperature (T_{75}), 90% weight loss temperature (T_{90}) and the temperature at which the sample stop degradation (T_{stop}) are listed in Table 1.

The thermal degradation data refers to all weight lose temperature of chitosan-*g*-AEMA which are higher than that of the prepared pure chitosan. This result could be attributed to the high moisture content of the chitosan and to the mobility limitation of the grafted AEMA polymer [31,32].

3.2. Grafting ratio of AEMA onto chitosan nanoparticles

Effect of chitosan/monomer ratio on the grafting yield of AEMA monomer onto chitosan nanoparticles was studied

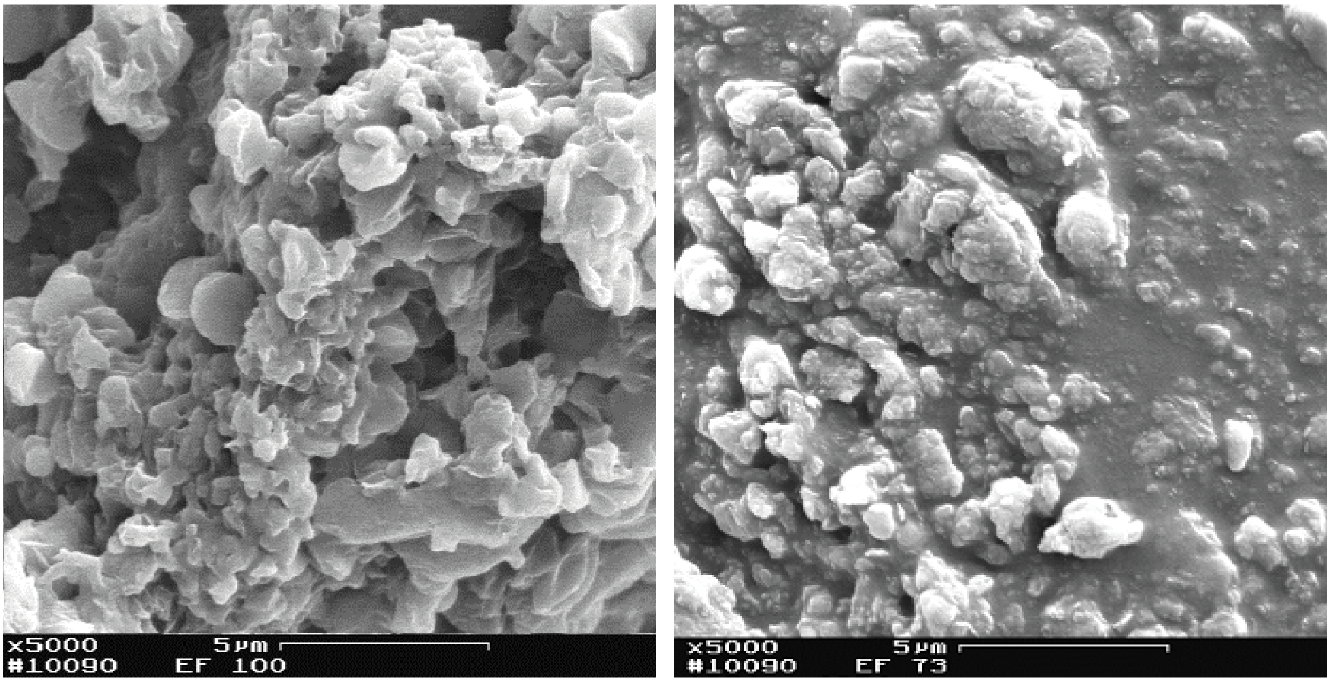

(A)

(B)

Fig. 3. SEM of the prepared (A) chitosan and (B) chitosan-*g*-AEMA.

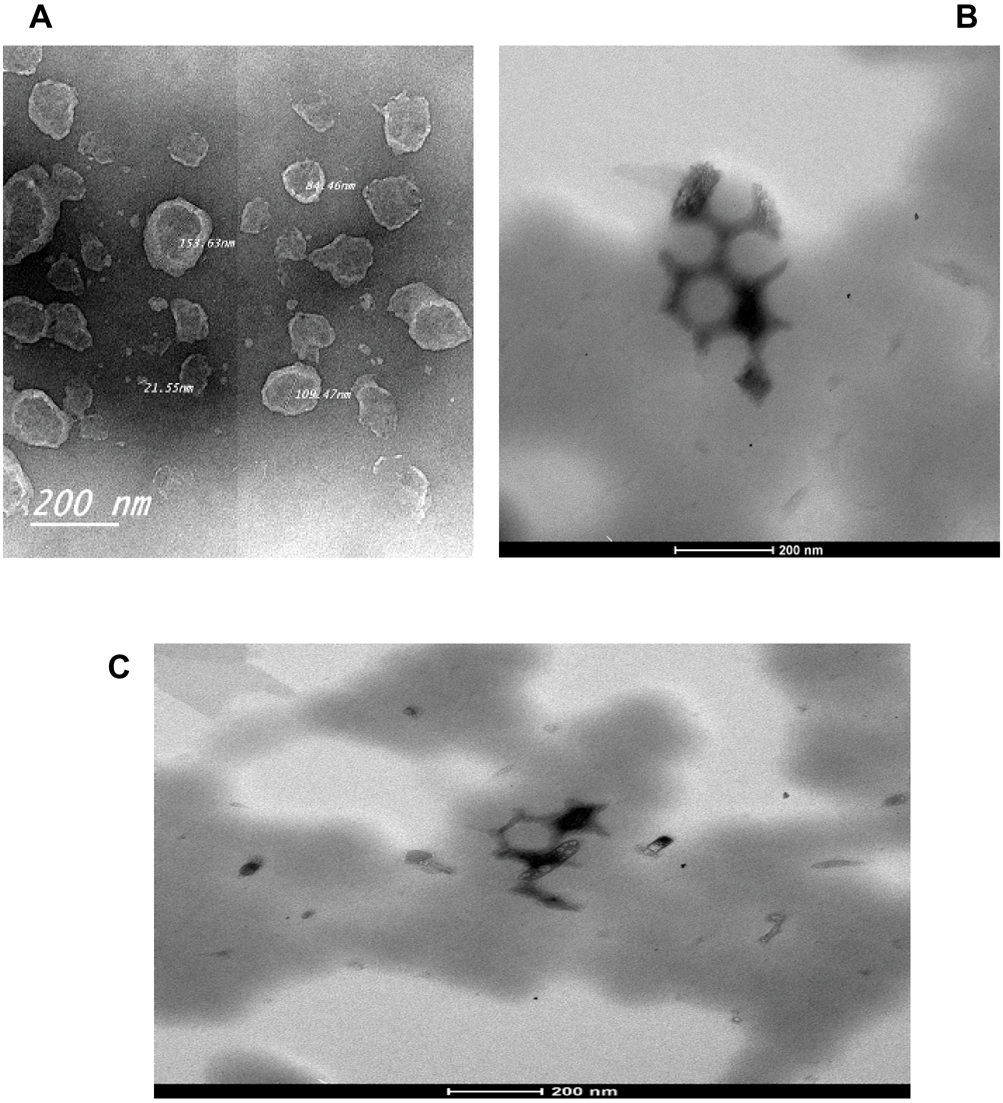

Fig. 4. TEM of the prepared (A) chitosan, (B) chitosan-*g*-AEMA and (C) chitosan-*g*-AEMA loaded Cr(VI).

and illustrated in Fig. 7. It is clear that the increasing of monomer ratio led to increasing in the grafting yield till reaching 52% with chitosan/AEMA ratio 2:1. The increasing in the grafting yield with increasing monomer ratio could be due to the rising in, the availability of growing polymer chains [33].

3.3. *Factors affecting Cr(VI) adsorption using chitosan and chitosan-g-AEMA*

3.3.1. *Effect of pH value*

The effect of pH on the adsorption percentage of Cr(VI) was studied at different pH (2–8), for 120 min using 0.2 g adsorbent dose and 100 mL of 1×10^{-3} mol L^{-1} Cr(VI) solution at 30°C (Fig. 8).

It is clear that, the removal efficiency percentage of Cr(VI) was increased rising the pH 3–6. Maximum removal percentage of Cr(VI) was attained at pH 6 due to decreasing in competition between H^+ and Cr(VI) ions by decreasing the positively charged group with increasing pH value in acidic range [34].

The decrease in removal efficiency percentage at pH > 6 is due to the formation of soluble hydroxide complexes with Cr(VI) ions [14].

The lower removal efficiency percentage values of Cr(VI) at pH 2 are due to the reduction of Cr(VI) to Cr(III) [35].

3.3.2. *Effect of adsorbent dose*

The effect of adsorbent dose on the removal efficiency percentage of Cr(VI) ions was investigated at pH 6, for 120 min using different doses from chitosan and chitosan-*g*-AEMA adsorbents in 100 mL of 1×10^{-3} mol L^{-1} Cr(VI) solution, at 30°C, and the results are illustrated in Fig. 9.

The data of Fig. 7 show that Cr(VI) ions removal efficiency percentage (in case of the types of adsorbents) is directly proportional with the amount of adsorbent dose. This behavior could be attributed to the increase in adsorbent dose, which

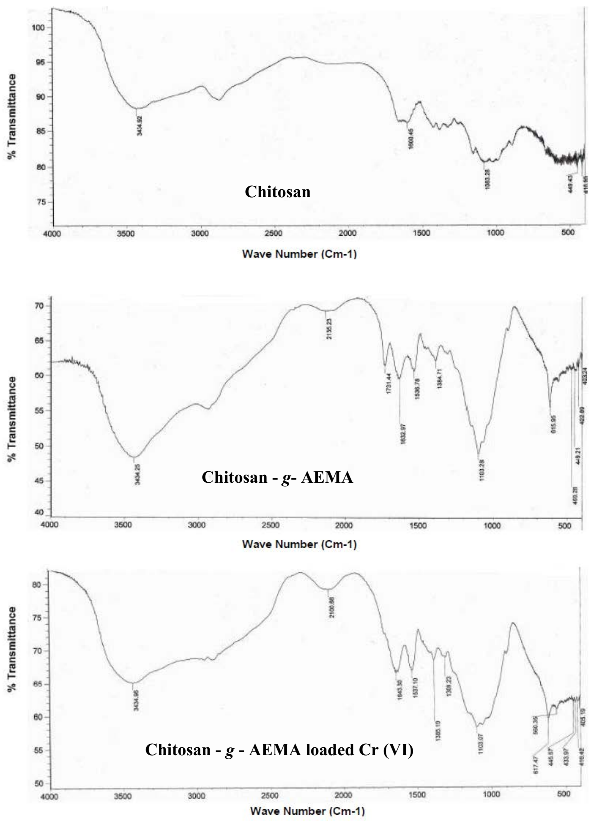

Fig. 5. FTIR analysis of the prepared chitosan, chitosan-*g*-AEMA and chitosan-*g*-AEMA loaded Cr(VI).

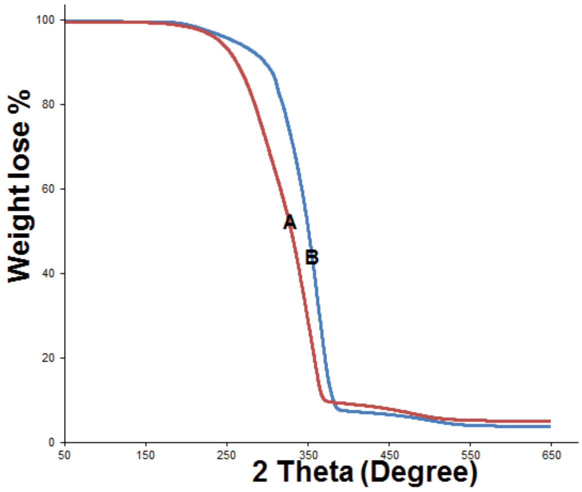

Fig. 6. TGA analysis of the prepared (A) chitosan and (B) chitosan-*g*-AEMA.

Table 1
TGA data obtained for chitosan and chitosan-*g*-AEMA

Temperature	Chitosan	Chitosan-*g*–AEMA
T_{start}	240	252
T_{10}	258	290
T_{25}	283	320
T_{50}	325	348
T_{75}	348	361
T_{90}	363	377
T_{stop}	376	387

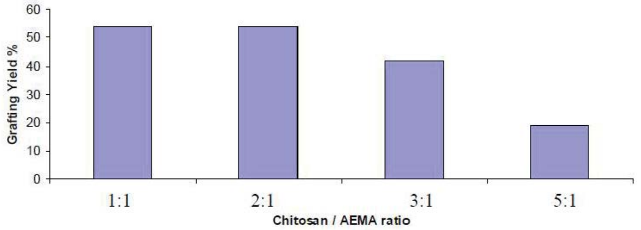

Fig. 7. Effect of chitosan/AEMA ratio on the grafting yield of AEMA onto chitosan.

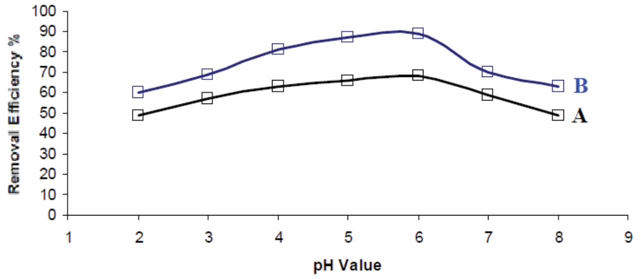

Fig. 8. Effect of pH value on the Cr(VI) removal efficiency percentage using (A) chitosan and (B) chitosan-*g*-AEMA adsorbents.

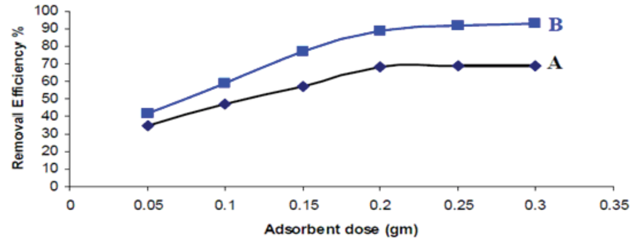

Fig. 9. Effect of adsorbent dose on the Cr(VI) removal efficiency percentage using (A) chitosan and (B) chitosan-*g*-AEMA adsorbents.

leads to an increase in the adsorption surface area giving more available adsorption active sites [36].

3.3.3. *Effect of adsorption time*

The effect of adsorption time (15–180 min) on the removal efficiency percentage of Cr(VI) was investigated at pH 6 using 0.2 g of adsorbent dose (chitosan and chitosan-*g*-AEMA) in 100 mL of 1 × 10^{-3} mol L^{-1} Cr(VI) at 30°C (Fig. 10).

The data illustrate that Cr(VI) removal efficiency percentage increased by increasing the adsorption contact time where equilibrium adsorption was observed at 120 min contact time for chitosan-*g*-AEMA and at 150 min with chitosan adsorbent. This figure, also indicates that the initial Cr(VI) removal rate was fast due to the high availability of adsorbent doses. Afterword, the rate of adsorption was decreased due to the limitation of vacant active adsorbent sites on the two types of adsorbent surface [37].

3.3.4. *Effect of adsorption temperature*

The effect of adsorption temperature (25°C–40°C) on the removal efficiency percentage of Cr(VI) ions for 120 min from its solution was investigated at pH 6, using 0.2 g of adsorbent dose from chitosan and chitosan-*g*-AEMA adsorbents in 100 mL of 1 × 10^{3} mol L^{-1} Cr(VI) solution.

The data illustrated that the temperature does not have a noticeable effect on the adsorption efficiency percentage of Cr(VI) using chitosan or chitosan-*g*-AEMA. The adsorption efficiency percentage was around the value of 89% at all the studied temperature range.

3.3.5. *Effect of Cr(VI) ion concentration*

The initial concentration of metal ions is an important factor to overcome the oppositions and resistance of ion transfer from solution to the adsorbent material.

Cr(VI) adsorption efficiency percentage was determined by using100 mL of various Cr(VI) ions concentrations (1 × 10^{-2} mol L^{-1} to 1 × 10^{-4} mol L^{-1}) at pH 6, for 120 min using 0.2 g from chitosan and chitosan-*g*-AEMA adsorbents at 30°C (Fig. 11).

From the data, it is clear that the removal efficiency percentage of Cr(VI) reached to about 97% in case of chitosan-*g*-AEMA with Cr(VI) concentration 1 × 10^{-4}mol L^{-1}. It is also obvious that there is an inverse relation between the initial Cr(VI) ion concentration and the removal efficiency percentage. This could be due to the limitation of adsorption active sites relative to the competing ions [8].

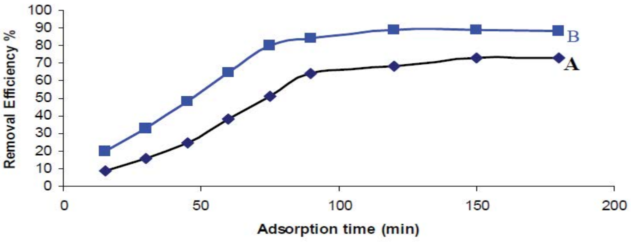

Fig. 10. Effect of adsorbent time on the Cr(VI) in removal efficiency percentage using (A) chitosan and (B) chitosan-*g*-AEMA adsorbents.

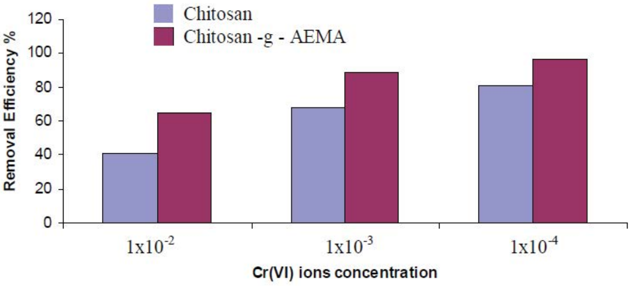

Fig. 11. Effect of initial Cr(VI) concentration in removal efficiency percentage using chitosan and chitosan-*g*-AEMA adsorbents.

In all factors studied including pH value, adsorbent dose, adsorption time, adsorption temperature, and Cr ions concentration, and from the data illustrated in Figs. 8–11. It is clear that the percentage of Cr(VI) removal using chitosan-*g*-AEMA is more than that using chitosan nanoparticles at all studied factors. This is due to the increase in the number of amino function groups by incorporation of AEMA polymer which led to increase in the active sites (N^+) formed in acidic solution and increases the adsorption capacity of Cr(VI).

3.4. *Adsorption isotherms*

The equilibrium adsorption isotherm of Cr(VI) using both chitosan and chitosan-*g*-AEMA is represented by Fig. 12.

The obtained results are well confirmed by Langmuir isotherm model. The Freundlich model is poorly fitted with the obtained data.

The Langmuir constants and coefficients listed in Table 2 are calculated according to the following equation [38]:

$$C_e/Q_e = 1/Qb + C_e/Q \tag{3}$$

where C_e is the equilibrium concentration (mg/L); Q_e is the amount of metal ion adsorbed at equilibrium (mg/g); Q is the Langmuir constant related to adsorption capacity; b is the Langmuir constant related to energy of adsorption.

C_e/Q_e against C_e gave a straight line with slope $1/Q$ shown in Fig. 12 which indicate that the adsorption follow Langmuir isotherm [39].

From the obtained data, it is clear that chitosan-*g*-AEMA has higher values of Q and b than the chitosan nanoparticle. This result could be attributed to the interaction force

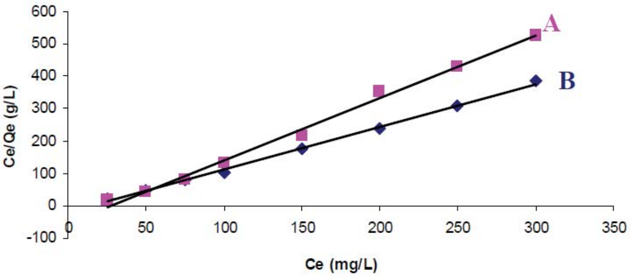

Fig. 12. Langmuir isotherm for sorption of Cr(VI) on (A) chitosan and (B) chitosan-*g*-AEMA.

Table 2
The Langmuir constants and correlation coefficients for adsorption of metal ions from aqueous solution using different adsorbents

Chitosan			Chitosan-*g*-AEMA		
Q	b	R^2	Q	b	R^2
0.511776	0.035	0. 9743	0.746887	0.0537	0. 983

between the sorbent and metal where the chelating bond between the tertiary amino group in chitosan-*g*-AEMA and Cr metal ion is stronger than the chelating bond between the primary amino group in chitosan and Cr metal ion [40].

4. Conclusion

Chitosan nanoparticles with particle size about 84 nm were successfully prepared in TPP aqueous solution and characterized by FTIR, SEM and TEM analyses.

The prepared chitosan nanoparticles was grafted with AEMA monomer using KPS/NaBS redox initiation system producing chitosan-*g*-AEMA with grafting percentage 52% in case of 2:1 chitosan/AEMA ratio.

The grafting process was confirmed by FTIR and the prepared grafted polymer was characterized by SEM, TGA and TEM analyses.

The prepared chitosan and chitosan-*g*-AEMA have been used in adsorption of Cr(VI) ions from its K_2CrO_4 solution in different pH values, adsorbent dose, adsorption time, adsorption temperature and Cr ion concentration.

The data showed that at all factors studied the percentage of Cr(VI) removal of chitosan-*g*-AEMA is more than that using chitosan nanoparticles.

The equilibrium isotherm of Cr(VI) adsorption using both chitosan and chitosan-*g*-AEMA and the obtained results are well described by Langmuir isotherm model.

Acknowledgment

The author would like to acknowledge the University of Tabuk for the financial support under research project number S-0020-1438.

References

[1] M. Naushad, T. Ahamad, B.M. Al-Maswari, A.A. Alqadami, S. M. Alshehri, Nickel ferrite bearing nitrogen-doped mesoporous carbon as efficient adsorbent for the removal of highly toxic metal ion from aqueous medium, Chem. Eng. J., 330 (2017) 1351–1360.

[2] M.R. Hoffmann, S.T. Martin, W. Choi, D.W. Bahnemannt, Environmental applications of semiconductor photocatalysis, Chem. Rev., 95 (1995) 69–96.

[3] G. Sharma, M. Naushad, A.H. Al-Muhtase, A. Kumar, M.R. Khan, S. Kalia, M. Bala, A. Sharma, Fabrication and characterization of chitosan-crosslinked-poly(alginic acid) nanohydrogel for adsorptive removal of Cr(VI) metal ion from aqueous medium, Int. J. Biol. Macromol., 95 (2017) 484–493.

[4] R. Jayakumar, M. Prabaharan, R.L. Reis, J.F. Mano, Graft copolymerized chitosan—present status and applications, Carbohydr. Polym., 62 (2005) 142–158.

[5] M. Siahkamari, A. Jamali, A. Sabzevari, A. Shakeri, Removal of lead(II) ions from aqueous solutions using biocompatible polymeric nano-adsorbents: a comparative study, Carbohydr. Polym., 157 (2017) 1180–1189.

[6] T.V. Nguyen, T.T. Nguyen, S. Wang, T.P. Khanh Vo, A.D. Nguyen, Preparation of chitosan nanoparticles by TPP ionic gelation combined with spray drying, and the antibacterial activity of chitosan nanoparticles and a chitosan nanoparticle–amoxicillin complex, Res. Chem. Intermed., 43 (2017) 3527–3536.

[7] J. Gu, K. Al-Bayati, E.A. Ho, Development of antibody-modified chitosan nanoparticles for the targeted delivery of siRNA across the blood-brain barrier as a strategy for inhibiting HIV replication in astrocytes, Drug Delivery Trans. Res., 7 (2017) 497–506.

[8] A. Janus, A. Pelfrene, S. Heymans, C. Deboffe, F. Douay, C. Waterlot, Elaboration, characteristics and advantages of biochars for the management of contaminated soils with a specific overview on *Miscanthus* biochars, J. Environ. Manage., 162 (2015) 275–288.

[9] M. Inyang, E. Dickenson, The potential role of biochar in the removal of organic and microbial contaminants from potable and reuse water: a review, Chemosphere, 134 (2015) 232–249.

[10] M.K. Kim, K.S. Sundaram, G.A. Iyengar, K.P. Lee, A novel chitosan functional gel included with multiwall carbon nanotube and substituted polyaniline as adsorbent for efficient removal of chromium ion, Chem. Eng. J., 267 (2015) 51–63.

[11] A. Heidari, H. Younesi, Z. Mehraban, H. Heikkinen, Selective adsorption of Pb(II), Cd(II), and Ni(II) ions from aqueous solution using chitosan-MAA nanoparticles, Int. J. Biol. Macromol., 61 (2013) 251–263.

[12] L. Li, L. Fan, M. Sun, H. Qiu, X. Li, H. Duan, C. Luo, Adsorbent for chromium removal based on graphene oxide functionalized with magnetic cyclodextrin-chitosan, Colloids Surf., B, 107 (2013) 76–88.

[13] Y. Zhou, B. Gao, A.R. Zimmerman, J. Fang, Y. Sun, X. Cao, Sorption of heavy metals on chitosan-modified biochar sand its biological effects, Chem. Eng. J., 231 (2013) 512–523.

[14] X. Huang, Y. Liu, S. Liu, X. Tan, Y. Ding, G. Zeng, Y. Zhou, M. Zhang, S. Wang, B. Zheng, Effective removal of Cr(VI) using β-cyclodextrin–chitosan modified biochars with adsorption/reduction bifunctional roles, RSC Adv., 6 (2016) 94–106.

[15] T. Ahamad, M. Naushad, B.M. Al-Maswari, J. Ahmed, Z.A. AL-Othman, S.M. Alshehri, A.A. Alqadami, Synthesis of a recyclable mesoporous nanocomposite for efficient removal of toxic Hg^{2+} from aqueous medium, J. Ind. Eng. Chem., 53 (2017) 268–275.

[16] P. Evangelopoulos, E. Kantarelis, W. Yang, W. Blasiak, Investigation of the thermal decomposition of printed circuit boards (PCBs) via thermogravimetric analysis (TGA) and analytical pyrolysis (Py–GC/MS), Fuel, 122 (2014) 119–132.

[17] J. Zhu, S. Wei, H. Gu, S.B. Rapole, Q. Wang, Z. Luo, N. Haldolaarachchige, D.P. Young, Z. Guo, One-pot synthesis of magnetic graphene nanocomposites decorated with core@double-shell nanoparticles for fast chromium removal, Environ. Sci. Technol., 46 (2012) 977–989.

[18] S. Debnath, A. Maity, K. Pillay, Magnetic chitosan-go nanocomposite: synthesis, characterization and batch adsorber design for Cr(VI) removal, J. Environ. Chem. Eng., 2 (2014) 963–973.

[19] M.R. Gandhi, S. Meenakshi, Preparation of amino terminated polyamidoamine functionalized chitosan beads and its Cr(VI) uptake studies, Carbohydr. Polym., 91 (2013) 631–637.

[20] A.S.K. Kumar, C.U. Kumar, V. Rajesh, N. Rajesh, Microwave assisted preparation of n-butylacrylate grafted chitosan and its application for Cr(VI) adsorption, Int. J. Biol. Macromol., 66 (2014) 135–143.

[21] R. Singh, H. Dong, Q. Zeng, L. Zhang, K. Rengasamy, Hexavalent chromium removal by chitosan modified-bioreduced nontronite, Geochim. Cosmochim. Acta, 210 (2017) 25–41.

[22] B. Hastuti, A. Masykur, S. Hadi, Modification of chitosan by swelling and crosslinking using epichlorohydrin as heavy metal Cr (VI) adsorbent in batik industry wastes, Mater. Sci. Eng., 107 (2016) 12020.

[23] L. Zhang, H. Luo, P. Liu, W. Fang, J. Geng, A novel modified graphene oxide/chitosan composite used as anadsorbent for Cr(VI) in aqueous solutions, Int. J. Biol. Macromol., 87 (2016) 586–596.

[24] L. Qi, Z. Xu, Y. Li, X. Jiang, X. Han, In vitro effects of chitosan nanoparticles on proliferation of human gastric carcinoma cell line MGC803 cells, World J. Gastroenterol., 11 (2005) 5136–5249.

[25] F. Hafida, A.S. Hadj-Hamou, Preparation of chitosan-g-poly(acrylamide)/montmorillonite superabsorbent polymer composites: studies on swelling, thermal, and antibacterial properties, J. Appl. Polym. Sci., 131 (2014) 1–14, doi: 10.1002/APP.39747.

[26] K. Shaffei, A.B. Moustafa, W.S. Mohamed, Grafting emulsion polymerization of glycidyl methacrylate onto leather by chemical initiation system, J. Appl. Polym. Sci., 109 (2008) 3923–3934.

[27] E.M. Mahmoud, M.K. Obada, T.S. Kassem, Removal and speciation of chromium by static step-by-step deposition and extraction technique, Chem. Eng. J., 230 (2013) 210–219.

[28] X.F. Tan, Y.G. Liu, G.M. Zeng, X. Wang, X.J. Hu, Y.L. Gu, Z.Z. Yang, Application of biochar for the removal of pollutants from aqueous solutions, Chemosphere, 125 (2015) 70–82.

[29] A.S. Badran, H.E. Nasr, N.R. El-Halawany, W.S. Mohamed, Modification of natural leather by grafting emulsion copolymerization technique, Polym. Plast. Technol. Eng., 46 (2007) 79–90.

[30] C.Q. Qin, Y.M. Du, L. Xiao, Effect of hydrogen peroxide treatment on the molecular weight and structure of chitosan, Polym. Degrad. Stab., 76 (2002) 211–218.

[31] S.A. Ali, W.S. Mohamed, Kinetic and equilibrium studies of waste polyethylene doped nanocomposite for dyestuffs removal, Global J. Pure Appl. Chem. Res., 3 (2015) 1–9.

[32] S.M. Nomanbhay, K. Palanisamy, Removal of heavy metal from industrial wastewater using chitosan coated oil palm shell charcoal, Electron. J. Biotechnol., 8 (2005) 43–53.

[33] M. Shirmardi, A.R. Mesdghinia, A.H. Mahvi, S. Nasseri, R. Nabizadeh, Kinetics and equilibrium studies on adsorption of acid red 18 (azo–dye) using multiwall carbon nanotubes (MWCNs) from aqueous solution, J. Chem., 19 (2012) 2371–2384.

[34] W. Li, X. Liu, Q. Yang, N. Zhang, Y. Du, H. Zhu, Preparation and characterization of inclusion complex of benzyl isothiocyanate extracted from papaya seed *with* β-cyclodextrin, Food Chem., 184 (2015) 99–112.

[35] H. Cho, D. Oh, K. Kim, A study on removal characteristics of heavy metals from aqueous solution by fly ash, J. Hazard. Mater., 127 (2005) 187–195.

[36] D.L. Bond, S. Fendorf, Kinetics and structural constraints of chromate reduction by green rusts, Environ. Sci. Technol., 37 (2003) 2750–2757.

[37] M. Sivakami, T. Gomathi, J. Venkatesan, H.S. Jeong, S.K. Kim, P. Sudha, Preparation and characterization of nano chitosan for treatment waste waters, Int. J. Biol. Macromol., 57 (2013) 204–212.

[38] Y. Bin, V. Zhang, A. Shukl, S. Shyam, S. Kenneth, L. Dorris, The removal of heavy metal from aqueous solutions by sawdust adsorption—removal of copper, J. Hazard. Mater., 80 (2000) 33–42.

[39] I. Langmuir, The constitution properties and fundamental of solids and liquids. II, J. Am. Chem. Soc., 39 (1917) 1848–1906.

[40] M. Raoa, A.V. Parwatea, A.G. Bhole, Removal of Cr^{6+} and Ni^{2+} from aqueous solution using bagasse and fly ash, Waste Manage., 22 (2002) 821–830.